Article details

Yu M., Sediq A.S., Zhang S., Nejadnik M.R., Every H.A., Jiskoot W. & Witkamp G.-J. (2018), Towards the development of a supercritical carbon dioxide spray process to coat solid protein particles, Journal of Supercritical Fluids 141: 49-59.
Doi: 10.1016/j.supflu.2017.12.014

The Journal of Supercritical Fluids 141 (2018) 49–59

Contents lists available at ScienceDirect

The Journal of Supercritical Fluids

journal homepage: www.elsevier.com/locate/supflu

Towards the development of a supercritical carbon dioxide spray process to coat solid protein particles

Miao Yu[a,*], Ahmad S. Sediq[b], Shiduo Zhang[a], M. Reza Nejadnik[b], Hayley A. Every[c], Wim Jiskoot[b], Geert-Jan Witkamp[a]

[a] Department of Biotechnology, Delft University of Technology, Van der Maasweg 9, 2629 HZ, Delft, The Netherlands
[b] Division of Drug Delivery Technology, Cluster BioTherapeutics, Leiden Academic Centre for Drug Research (LACDR), Leiden University, Einsteinweg 55, 2333 CC Leiden, The Netherlands
[c] FeyeCon Development & Implementation B.V., Rijnkade 17-A, 1382 GS, Weesp, The Netherlands

GRAPHICAL ABSTRACT

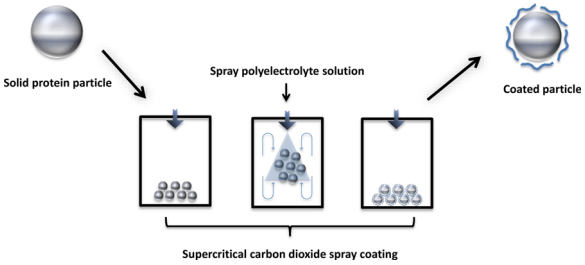

ARTICLE INFO

Keywords:
Supercritical carbon dioxide
Lysozyme
Dextran sulphate
Drug delivery systems
Proteins

ABSTRACT

The aim of this study was to develop a supercritical carbon dioxide ($scCO_2$) spray process to coat solid protein particles with a hydrophilic polymer. The final purpose is to manufacture drug particles exhibiting controlled release behaviour in patients. Lysozyme microparticles (about 20 μm) were suspended in a vessel into which a dextran sulphate (DS) solution was dispersed by $scCO_2$ via a nozzle. Upon interaction with the droplets, DS was deposited onto or mixed with suspended lysozyme particles. Particles of about 100 μm were obtained. The zeta-potential analysis and elemental analysis indicated that the top layer of the particles consisted of both lysozyme and DS. Some of the produced particulate materials showed retarded lysozyme release when exposed to water or phosphate buffered saline, holding promise for future production of controlled drug delivery systems for therapeutic proteins.

1. Introduction

Protein therapeutics are successfully applied to treat chronic and life-threatening diseases owing to their high specificity and potency. One drawback of these drugs is that they have to be administered parenterally, i.e., intravenously, subcutaneously or intramuscularly, and often require frequent injections or continuous infusion due to rapid clearance from the bloodstream [1]. One way to overcome this is to encapsulate these drugs in an implantable macroscopic or injectable microparticulate drug delivery system (DDS) from which they are slowly released after administration. However, the development of an effective DDS for proteins remains a challenge, as reflected by the low number of such products on the market [2–5].

Up to now, polymers such as polylactic acid (PLA) and poly(lactic-co-glycolic) acid (PLGA) have been used as carriers to encapsulate proteins [6]. The use of these polymers, however, comes with

* Corresponding author at: Hanze University of Applied Sciences, Zernikeplein 11, 9747 AS, Groningen, The Netherlands.
E-mail address: M.Yu@tudelft.nl (M. Yu).

https://doi.org/10.1016/j.supflu.2017.12.014
Received 3 October 2017; Received in revised form 3 December 2017; Accepted 9 December 2017
Available online 11 December 2017
0896-8446/

disadvantages such as denaturation of proteins during production because of contact with the polymers, organic solvents and interfaces, and the formation of acidic degradation products causing a local drop in pH during release, leading to protein aggregation and incomplete protein release [7].

As an alternative to the conventionally used polymers, hydrophilic polymers could be employed, which are more protein friendly. In the past decades, the interest for natural or chemically modified polysaccharide-based polymers in the development of controlled drug delivery systems has increased due to their stability, safety, non-toxicity, hydrophilicity and biodegradability [8–12]. Charged polymers like polyelectrolytes are widely applied in food, biotechnology, pharmaceutical and cosmetic industry and are used as dispersing agent, purification reagent, conditioner, etc. [13–15]. In addition to these applications, polyelectrolytes have been studied as coating material for food and pharmaceutical purposes [16,22] with a number of advantages [18]. One of them is that the coating process can be performed in an aqueous environment under mild conditions without the use of organic solvents, which helps to preserve the bioactivity of sensitive biomolecules like proteins. Proteins can be easily incorporated within polyelectrolyte materials, because they are natural polyelectrolytes themselves, and due to their amphotericity the protein charge can be changed through a well-chosen shifted pH [19,20]. The complex formation with the polyelectrolyte might however affect the protein structure and activity [18].

For the purpose of controlled protein release, polyelectrolytes may be employed to build up multi-layer coatings (LbL (layer by layer)) by the application of alternating positively-charged and negatively-charged polyelectrolytes [16]. Compared with conventional encapsulation methods like emulsion-solvent extraction/evaporation [6,21], i) LbL coating does not require harmful organic solvents; ii) avoids the use of thermal evaporation steps which can damage the protein; iii) the protein release behaviour can be adjusted by selecting the proper types of polyelectrolytes, arranging the number of coating layers and modifying the interactions among the charged polymers [16,18,22].

It would be even more advantageous if we were able to carry out protein coating by polyelectrolytes in supercritical carbon dioxide ($scCO_2$). $ScCO_2$ has been examined as a solvent to process protein pharmaceuticals because of its mild critical temperature and pressure, nontoxicity, the absence of solvent/water interfaces and it does not leave traces in the product [23]. $ScCO_2$ can be applied as a drying medium for the proteins and for the production of formulated protein-containing microparticles [24]. In addition, via changes in the kinetics of CO_2 depressurization, the particle morphology can be controlled to generate materials of variable density and surface roughness [25].

Protein encapsulation for controlled release using $scCO_2$ has been investigated before [25–32]. In these studies, hydrophobic materials such as PLA, PLGA and lipids, were usually selected as the coating materials, and in some cases organic solvents were applied. As far as we know, there have been no studies on protein coating using polyelectrolytes in $scCO_2$ processes.

The selection of polymer-based coating methods for microparticle encapsulation depends on many factors like the desired final coating layer thickness and product particle size. Spraying coating involves bringing core particles in contact with the sprayed polymer-containing droplets. Conventionally, this coating process provides many advantages such as uniform coating, coating layer thickness control, and multilayer coating [33,34]. By combining the aforementioned advantages of spray coating and $scCO_2$ processes including drying under mild conditions, a novel approach can be developed for producing controlled release protein formulations.

This paper reports on an exploratory study aimed at evaluating the possibility of developing a $scCO_2$ process to coat dry protein-containing hydrophilic micro-sized core particles with a shell of a single type of biodegradable and hydrophilic polyelectrolyte. In this study lysozyme was chosen as a model protein and dextran sulphate (DS) as the coating material. The obtained dry microparticles were characterised for particle morphology, residual moisture content, protein release profile, zeta-potential and surface composition.

2. Experimental

2.1. Materials and preparations of feed solutions

Hen egg white lysozyme (~70000 U/mg, Sigma-Aldrich, St. Louis, USA) was dissolved in ultrapure water (purified using a Milli-Q ultrapure water system, Millipore™, Molsheim, France) and was used for the production of lysozyme core microparticles via a $scCO_2$ spray drying process (see 2.2). DS (dextran sulphate) (Sigma-Aldrich, St. Louis, USA) solution (10% w/w) was also prepared in ultrapure water for the spray coating onto lysozyme core particles. For the *in vitro* study on the protein release performance, a phosphate buffer was prepared with phosphate salts (Na_2HPO_4 and NaH_2PO_4) and sodium chloride (NaCl) (Sigma-Aldrich, St. Louis, USA). All liquid formulations were filtered through a 0.22 µm cellulose filter (Whatman, GE Healthcare, Freiburg, Germany) before experiments. For all the $scCO_2$ related processes, CO_2 (99% purity) was purchased from Linde group (Linde Gas Benelux BV, The Netherlands).

2.2. Preparation of lysozyme core particles

Prior to the coating experiments, solid spray-dried lysozyme core microparticles were prepared according to previous methods, with a uniform spherical morphology with a relatively narrow size distribution [24]. Briefly described, lysozyme solution (10% w/w) was prepared with ultrapure water as the solvent. An amount of 20 ml of this solution was sprayed into a 4-litre $scCO_2$ spray drying vessel via a co-axial nozzle (inner liquid diameter 0.05 cm and outer $scCO_2$ diameter 0.24 cm) at a solution flow rate of 0.2 ml/min, $scCO_2$ flow rate of 30 kg/h, a temperature of 37 °C and a pressure of 130 bar.

2.3. Particle suspension & spray coating (PSSC) process

2.3.1. Experimental set-up

Fig. 1 illustrates the scheme of the $scCO_2$ spray coating process. The $scCO_2$ was supplied by a diaphragm pump (LEWA, Leonberg, Germany) to a half-litre pressure vessel.

During the process, an amount of solid lysozyme core particles was placed in the vessel, followed by warming and pressurization with the CO_2. With the help of the agitator (a shaft with both disk turbine and pitched-blade turbine mounted), the lysozyme powder was suspended in the vessel. DS solution was fed into the vessel by a high-pressure piston pump (ISCO, Lincoln, USA). By means of a nozzle-contained T-mixer in which single-hole nozzles were placed, DS solution and $scCO_2$ were mixed and sprayed into the vessel, which is explained in detail below. Products from the process were collected at the bottom of the vessel where paper filters were placed. The paper filter was prepared by cutting normal printing paper fitting the inner bottom of the vessel. Ten layers of the paper were fixed at the bottom of the vessel. The paper filter remained intact after the spray coating process.

In order to conveniently describe the process developed in our study, it is named particle suspension & spray coating (PSSC) process.

2.3.2. Nozzle configurations

These experiments aimed to investigate the influence of different nozzle configurations on the dispersion of the DS liquid. Four types of nozzle arrangements in the T-mixer, named C1, C2, C3 and C4, respectively, as shown in Fig. 2, were tested to evaluate the influence of the nozzle configuration on the dispersion of polymer droplets. C1, C2 and C3 had configurations that bend the $scCO_2$ flow while C4 had a configuration of straight flow. First the vessel was filled with CO_2. In all

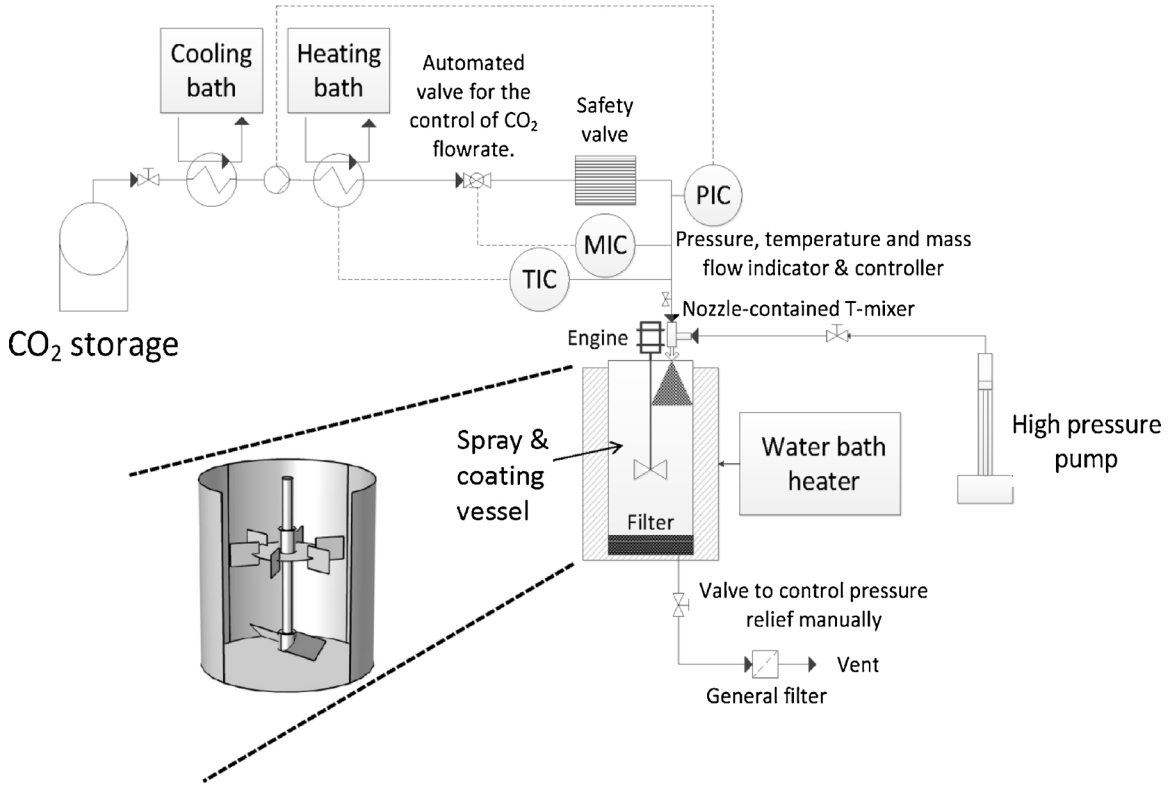

Fig. 1. Sketch of the PSSC experimental set-up. $ScCO_2$ was pressurized and heated to supercritical state (in this study to 130 bar and 37 ° C), and introduced into the spray & coating vessel via a nozzle-contained T-mixer, in which the high-speed $scCO_2$ flow atomizes the DS solution (introduced by an ISCO pump) into tiny droplets. A disk turbine and pitched-blade turbine were placed in the spray & coating vessel to mix the core particles (placed in the vessel before pressurization) and the atomized polymer droplets.

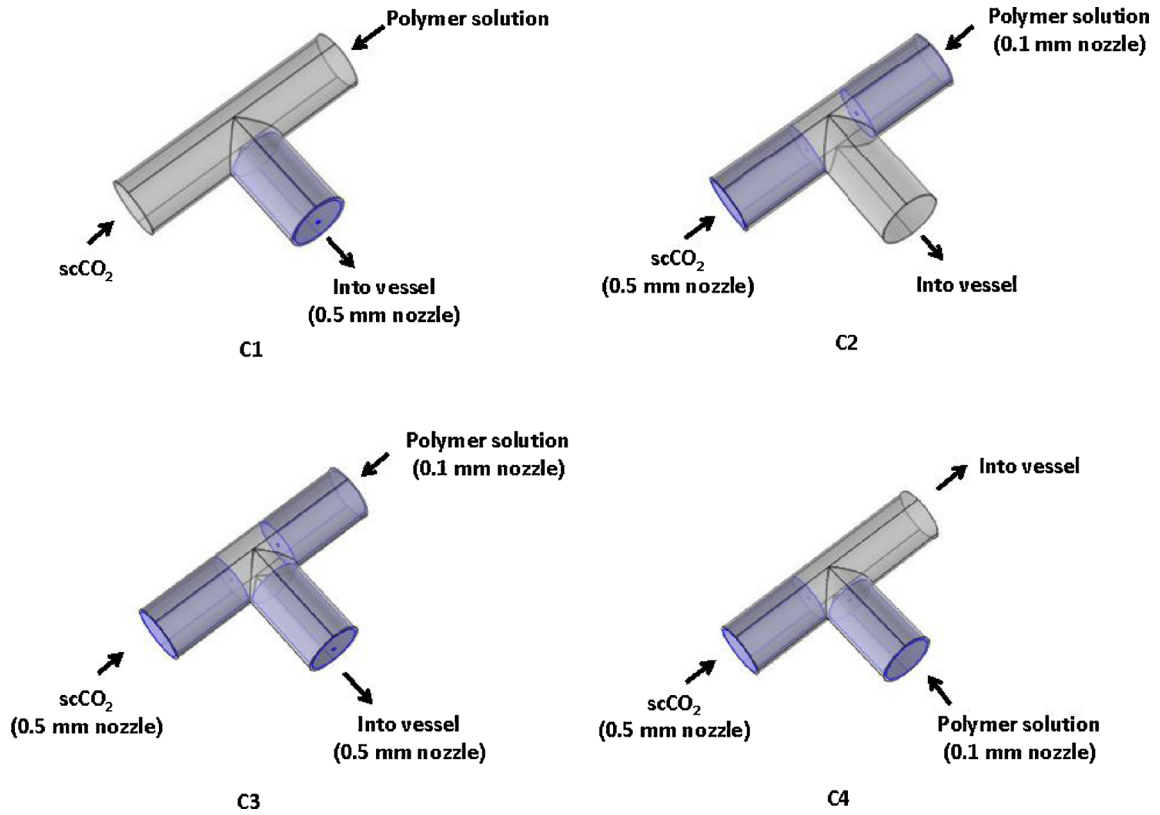

Fig. 2. Scheme of the configurations (C1, C2, C3 and C4) of the nozzle-contained T-mixers applied in the PSSC process. Nozzles (shown as the hole embedded in the blue cylinders) with different sizes were connected in T-mixers made by cylinder tubes (about 9.5 mm inner diameter). The arrows show the direction of the fluids. The nozzle wall plate thickness was about 1- 2 mm (For interpretation of the references to colour in this figure legend, the reader is referred to the web version of this article.)

Table 1
Operating conditions used for the PSSC process.

Sample	DS concentration (w/w)	Flow rate (ml/min)	Nozzle configuration
Control	0%	1	C4
S1	10%	0.2	C4
S2	10%	0.5	C4
S3	10%	1	C4

these experiments, a $scCO_2$ flow rate of 300 g/min was applied during the spraying process. The operating conditions were maintained at a temperature of 37 °C and a pressure of 130 bar. Ten ml DS solution (10% w/w) was introduced into the vessel at a flow rate of 0.2 ml/min. The agitator rotated at a rate of 500 rpm. The liquid drops were dried as the result of quick mass transfer between water and $scCO_2$. After the injection of DS solution, the vessel was flushed for 30 min at 300 g/min with fresh $scCO_2$ to avoid making products with a high residual moisture content.

2.3.3. Processing conditions

Several experiments were performed to evaluate the applicability of the PSSC process for the coating of lysozyme core particles (see Table 1).

During these experiments, 1 g lysozyme core particles was suspended in $scCO_2$ in the half-litre pressure vessel with an agitation at 500 rpm, which is higher than the minimum required agitation speed (about 170 rpm) for solid suspension based on an classical equation pioneered by Zwietering [35]. The vessel was pressurized with $scCO_2$, and was regulated at a flow rate of 300 g/min at 130 bar and 37 °C. Once the pressure was stable, 10 ml DS solution (10% w/w) was atomized into the vessel together with the $scCO_2$ via the T-mixer nozzle. The overall mass ratio of lysozyme to DS during this process was 1:1. The feeding rate of DS was varied to learn about the influence of this parameter on the coating of the core particles. After the injection of DS solution, the vessel was flushed with $scCO_2$ (300 g/min) for 30 min with agitation for further contact of particles and sprayed DS droplets, as well as the removal of the residual water from the vessel. After depressurization, the product was recovered from the filter on the bottom of the vessel for further analysis.

The samples collected with different operating conditions are named as Control, S1, S2 and S3, respectively.

2.4. Particle characterisation

2.4.1. Particle size distribution

DS solution was atomized using different nozzle configurations (see 2.3.2) and dried in the vessel. The particle size distribution of the spray dried DS microparticles was measured by the tri-laser diffraction light scattering technique using a Microtrac S3500 particle analyser (Microtrac S3500, Montgomeryville, USA). Microtrac FLEX software (version 10.3.14) was used to calculate the particle size distribution. The device offers two operating modes, i.e., a wet (fluid dispersion) mode and a dry (air dispersion) mode. In the wet mode, the liquid-particle shear and implemented sonification help the homogenisation of the samples; in the dry mode, air flow is used for powder dispersion. In terms of the measurement size range, the wet mode has a lower detection limit (about 0.02 um) than the dry mode (about 0.2 um). The wet mode seems to be better for particle size determination. However, a proper liquid medium is needed to avoid sample dissolution and sample interaction.

Methanol was used as the liquid medium as it is a non-solvent for DS. Sonification (2 min at an ultrasound power of 25 W) was used to improve the homogeneity of the suspension. A refractive index value of 1.59 for particles and 1.33 for methanol was used. A measurement size range of 0.02–1408 μm was selected. Each sample was measured in duplicate and the averaged particle size distribution (each measurement itself was the average of triplicated recycling measurements) was reported.

The size distribution of particles obtained from the PSSC process was measured by the same device in the dry (air dispersion) mode to maintain the solid state of the collected particles and to avoid re-dissolution (as lysozyme can be dissolved in solvents like methanol) and unexpected inter-particle interaction. During the measurement, the dry powder was blown through the beam by means of pressure and sucked into a vacuum cleaner. During the dry mode measurement, the size range of 0.2–1408 um was used and each sample was measured once.

2.4.2. Scanning electron microscope and energy dispersive spectroscopy

A scanning electron microscope (SEM), integrated with Energy Dispersive Spectroscopy (EDS) (JSM-6010LA, JEOL, Tokyo, Japan) was used to examine the morphology of the microparticles as well as the elemental composition of the microparticle surface. Conductive double sided tape was used to fix the particles to the specimen holder before sputtering them with a thin layer of Au-Pd. All the samples were analysed in map mode during EDS analysis, where the distribution and intensity of elements were measured in the scanned area and a summarised elemental composition of the scanned area was reported.

The EDS analysis was performed for lysozyme, DS, Control, S1, S2 and S3 at the accelerating voltages of 10 kV), counting rate higher than 1000 cps and dead time lower than 4%. Elemental carbon (C), nitrogen (N), oxygen (O) and sulphur (S) were measured as feature elements to distinguish lysozyme and DS. For the EDS analysis, at least 3 different particles were chosen for elemental composition analysis. The average values of the elemental compositions of the measured particles together with their standard deviations are reported.

The influence of different accelerating voltages on the detected elemental composition was investigated. S3 was selected for this measurement for its relatively high detected sulfur content (see 3.5). One particle of S3 was selected; three different positions on the particle were measured for elemental content in the sequence of 5, 10, 15 and 20 kV. The average value of the measured elemental compositions of the three detected positions under each accelerating voltage is reported.

2.4.3. Zeta-potential analysis

Zeta-potential measurements are commonly employed to determine whether the electrical charge on the surface of a particles is positive or negative, and is used as a means of monitoring the deposition of surface layers [36].

A polar liquid medium has to be used for the zeta-potential measurement. Zeta-potential of the product was measured in ethanol (rather than methanol to avoid the possible dissolution of lysozyme [37]), in which lysozyme and DS are only sparingly soluble, via electrophoretic light scattering (ELS) combined with phase analysis light scattering (PALS) (Zetasizer Nano ZS, Malvern Instruments, Malvern, UK). About 0.01 g sample powder was put in a cuvette filled with 1 ml ethanol, followed by immediate measurement. Refractive indices of 1.36 and 1.59 were used for ethanol and particles, respectively. A voltage of 5 V was applied during the measurement. Each sample was measured in triplicate and the mean zeta-potential value, standard deviation of the triplicated measurement and zeta-deviation, which reflects the width of the charge distribution obtained in the experiment [38] and was calculated by Malvern Zetasizer Software v7.11, were reported.

2.4.4. Moisture content analysis

The moisture content measurements of the samples were conducted with a Karl-Fischer coulometer (Metrohm 756F, Herisau, Switzerland). An amount of powder (about 0.01 g) was weighed in a chromatography vial, which was sealed after loading the powder, followed by the addition of 1 ml methanol. After half an hour water extraction by methanol, 0.1 ml of the water-methanol mixture was injected into the

coulometer sample chamber for analysis. The measurement was performed in triplicate and the average value with the standard deviation was reported as percentage of the sample weight (% w/w).

2.4.5. Protein concentration determination

The lysozyme concentration was determined with the use of a UV spectrophotometer (Agilent 8453, Agilent Technologies, Santa Clara, USA). The dissolved lysozyme sample was placed in a cuvette with path length of 1 cm and absorbance at 280 nm was measured. By using an extinction coefficient of 2.64 ml mg^{-1} cm^{-1} [39], the lysozyme concentration in the measured sample was calculated.

2.4.6. Protein load determination

In order to determine the total lysozyme content in the product particles (containing both lysozyme and DS), about 2 mg of powder was dissolved in 1 M NaCl solution (at room temperature), where it is assumed that all the protein-polyelectrolyte complexes would dissociate at this high ionic strength.

2.4.7. Protein release studies

Lysozyme release profiles were achieved with the following procedure: 0.13 g powder was added to a flask, along with 13 ml purified water, or phosphate buffered saline (PBS) (pH 7.4; 10 mM phosphate salts (Na_2HPO_4 and NaH_2PO_4); 150 mM NaCl). The release experiments were performed in an incubator-shaker at 37 °C and 200 rpm. At different time points (1 h, 1 day, 2 days and 4 days) 1.5 ml of the dissolution medium was transferred into an Eppendorf tube and simultaneously 1.5 ml of the corresponding fresh medium was added to the sample flask. After centrifugation for 15 min at 18000 x G, a UV spectrum of the supernatant was recorded.

3. Results

3.1. Configuration of nozzle-contained T-mixer

This section treats the performance of the tested nozzle configurations in the T-mixer with respect to DS droplet dispersion. One of the tested nozzle configurations was selected for the later PSSC process. DS solutions were sprayed by using the different nozzle configurations shown in Fig. 2. It was aimed to disperse DS liquids into droplets with a size smaller than the core particles, while avoiding the presence of droplets larger than the core particles (see 4.1.1 for discussions).

The number-based and volume-based size distributions of spray dried DS particles obtained with different nozzle configurations are shown in Fig. 3. The volume-based particle size is biased toward larger particles.

All the applied four nozzle configurations show comparable number-based particle size distributions with an average particle size of 5 μm. The spray-dried DS particles from C3 have the highest ratio (about 80%) of particles with a (volume-based) size larger than that of the core particles (about 90 μm (volume-based)) compared to the rest of nozzle configurations (C1: about 60%; C2: about 63% and C4: about 71%). During the experiments, a blockage of the outlet nozzle sometimes happened due to the rapid drying of tiny droplets by $scCO_2$ inside the T-mixer. Thus, it was better to avoid the nozzle positioned in the outlet of the T-mixer and C3 was not selected for the PSSC process.

Although there is a presence of large particles of about 1000 μm for C1 and C4, the number of these particles is minimal. To avoid the risk of outlet nozzle blockage, C1 was not selected for the PSSC process. The $scCO_2$ transport in C2 involves a bend in the tube, while for C4 the tubing is more straight, which is preferable with respect to avoiding hindrance and resistance encountered during $scCO_2$ transport. Therefore C4 was selected as the configuration for the droplet generation in the PSSC process.

3.2. Morphology and size distribution of particles obtained via the PSSC process

SEM was performed to study i) the morphology of the lysozyme core particles, which were produced via spray drying; ii) particles from the control experiment; and iii) particles formed after spray coating with DS in the PSSC process. The results are shown in Fig. 4. The used lysozyme core particles were spherical with an average diameter of about 20 μm. After the PSSC process, with either water (Control) or DS spraying, only a few original core particles were found back, and most particles seemed to consist of agglomerates of differently shaped sub-particles, mostly much larger than the core particles (up to hundreds of micrometres). Apparently some dissolution and reconstitution of the lysozyme had taken place.

It appeared that the sample S2 (where DS solution flowrate was 0.5 ml/min) consisted of agglomerates of a larger size than the other samples. However, these agglomerates consisted of sub-particles with a size similar to the particles in S1 (DS solution flowrate of 0.2 ml/min) and S3 (DS solution flowrate of 1 ml/min).

In the sample of S1, there were many 1–2 μm small particles deposited onto the surface of large particles, where in S2 and S3 such small particles were much less abundant. SEM images of S1 at higher magnification are provided in the supplementary materials (Supplementary figures and tables, Fig. 2).

Laser diffraction particle size analysis was performed to study the size of the sample particles relevant to the PSSC process. The results are shown in Fig. 5. The lysozyme core particles had an average size of about 20 μm (number-based). After the PSSC process, big particles (often agglomerates) of about hundreds of micrometre size were produced. Although the particles in S2 were visible with SEM as clusters of hundreds of microns, the measured particle size distribution (number-based) shows no significant increase in particle size compared to S1, and S3 was much bigger according to the size distribution. Apparently, the clusters are loose aggregates of smaller particles (sub-particles). The aggregates become separated during the particle analysis with air dispersion. As indicated by the size distribution (see Fig. 5), the Control and S3 samples apparently contain more large particles (i.e., size > 100 μm) than S1 and S2.

Although with SEM small particles could be observed (similar to the core particles, around 20 um) these small particles were not detected (e.g. in Control, S2 and S3) by the laser diffraction particle size distribution. It may be possible that during laser diffraction analysis the large particles overshadow the small ones during measurement, or the amount of small particles is not enough to induce signal intensity over the detection limit, as recently shown for PLGA microparticles [40].

3.3. Residual moisture content

It has been reported [24] that a residual moisture content below 3% should be low enough to maintain the chemical and/or conformational stability of protein products over time. However, the influence of water on the stability of proteins depends on the protein type and its formulation, thus it cannot be generalized for all situations.

In this study, the residual moisture content is also an indication of the humidity level in the vessel as a result of the DS spraying flowrate. The residual moisture content of the samples is shown in Table 2. The average moisture content of lysozyme core particles produced via $scCO_2$ spray drying was 2.5%, similar to the dried protein formulation moisture content as reported before [24]. For the Control sample as well as the products obtained via PSSC process with DS, moisture contents of about 3–5% were obtained. According to a T-test (performed via the Data Analysis toolbox of Excel 2010), the moisture contents of the samples S1 and S2 differed insignificantly from that of the lysozyme core particles. There was a statistically significant difference between the moisture content of the lysozyme core particles and S3 ($P < 0.05$), indicating a higher residual moisture content after

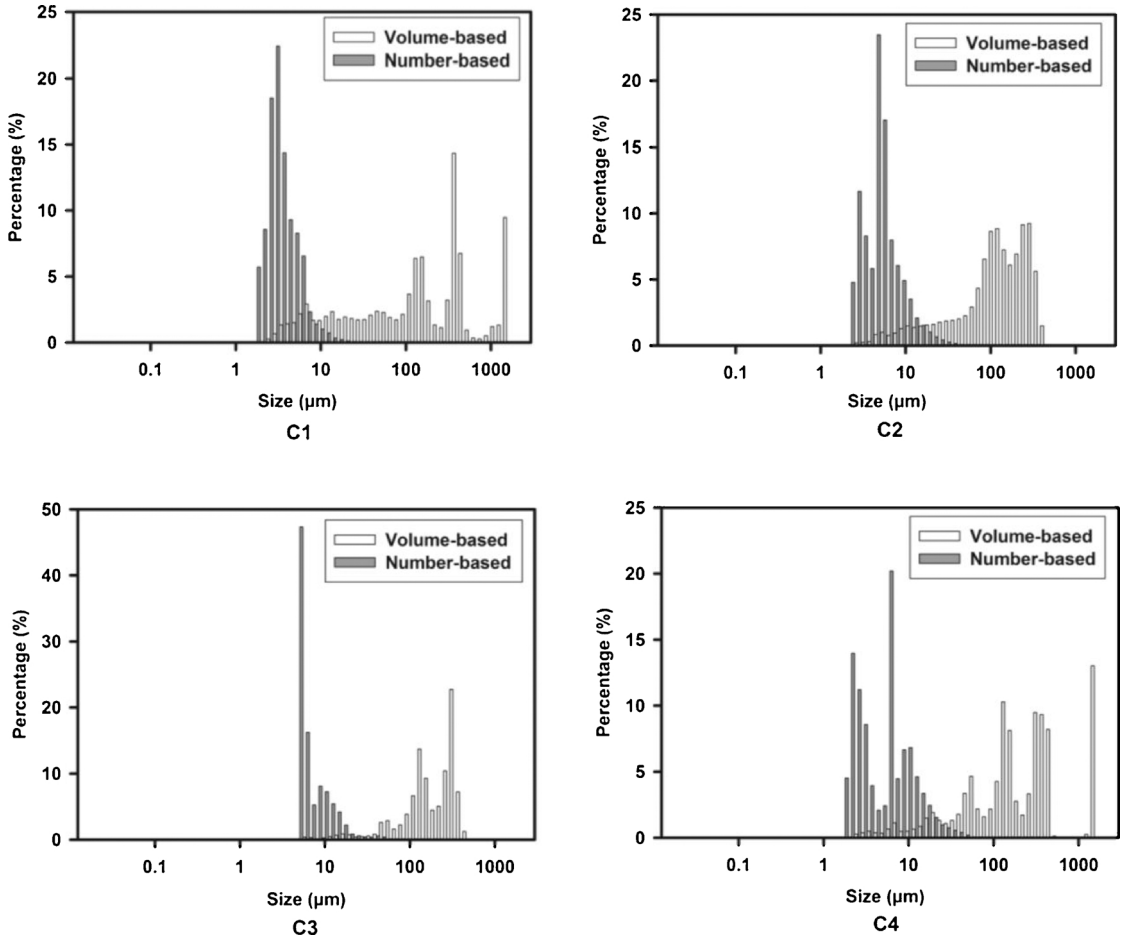

Fig. 3. Particle size distribution, measured in wet mode by laser diffraction, of spray dried DS which were produced via nozzle configurations C1, C2, C3 and C4 (see Fig. 2 and text for details). This particle size distribution is the average of duplicated measurements. The particle size distributions of each measurement are supplied in the supplementary materials of this paper (Supplementary figures and tables, Fig. 1).

the particle-droplet interaction at a higher DS flow rate. Moreover, S3 also shows a significant difference from that of the Control sample.

3.4. Zeta-potential

Table 3 shows the zeta-potential of lysozyme, DS, and products from the PSSC process. As expected, lysozyme displayed a positive mean zeta-potential, opposite to that of DS. Control samples from the PSSC process showed a positive mean zeta-potential, consistent with the results for the pure lysozyme. The DS-lysozyme products from the PSSC process all showed a negative mean zeta potential and S1 showed a more negative zeta-potential than S2 and S3.

Broad zeta deviations of the sample particles were observed, especially for the product of the PSSC process where the zeta deviation was even higher than the mean zeta-potential.

3.5. EDS analysis

Energy dispersive (X-ray) spectroscopy (EDS) analysis was conducted to evaluate the composition of the product particle top layer (a few μm depth) in a dry state after the PSSC process. Fig. 6 shows the elemental composition of lysozyme, DS and the samples obtained from the PSSC process, including the Control sample and the ones containing DS. Four elements, that is C, N, O and S, were selected as representative elements for the identification of materials in the product. In lysozyme, the S content was minimal with about 2% detected mass percentage where C and N dominated, as expected. In DS, N was a trace element where O and S contents were both higher than those in lysozyme, because of the presence of the hydroxyl groups and sulphate groups. The detected elemental compositions of lysozyme and DS are comparable with references [41,42]. The Control sample shows similar content of elements as lysozyme. In all the products from the PSSC process containing DS, the mass content of S and N falls in between that of lysozyme and DS. At 10 kV accelerating voltage, the EDS analysis can reach a penetration depth of a few micrometres into the sample [43]. Therefore, according to the EDS analysis, on the top layer of the product particles from the PSSC process, there was a combination of lysozyme and DS (as expected from a coating).

The product particles of S3 were (because of the relatively high sulphur content of S3) selected to be measured under different accelerating voltages to study the influence of this factor on the particle composition. The information is provided in the supplementary materials (Supplementary figures and tables, Fig. 3). According to the results, lysozyme was the dominating material of the detected particles with a mass ratio over 70%, and the calculated compositions of the detected particles differed slightly as function of accelerating voltage.

3.6. Protein release profile

The *in vitro* protein release profile of DS-encapsulated lysozyme particles obtained via PSSC process was examined. The sample S1 and S2 showed burst release in PBS of about 80–90% at 1 h (the first time point) without showing the expected controlled release behaviour. The lysozyme release profiles of S1 and S2 are provided in the supplementary materials (Supplementary figures and tables, Fig. 4). Only the protein release profile of Control and S3 sample are shown in Fig. 7. The

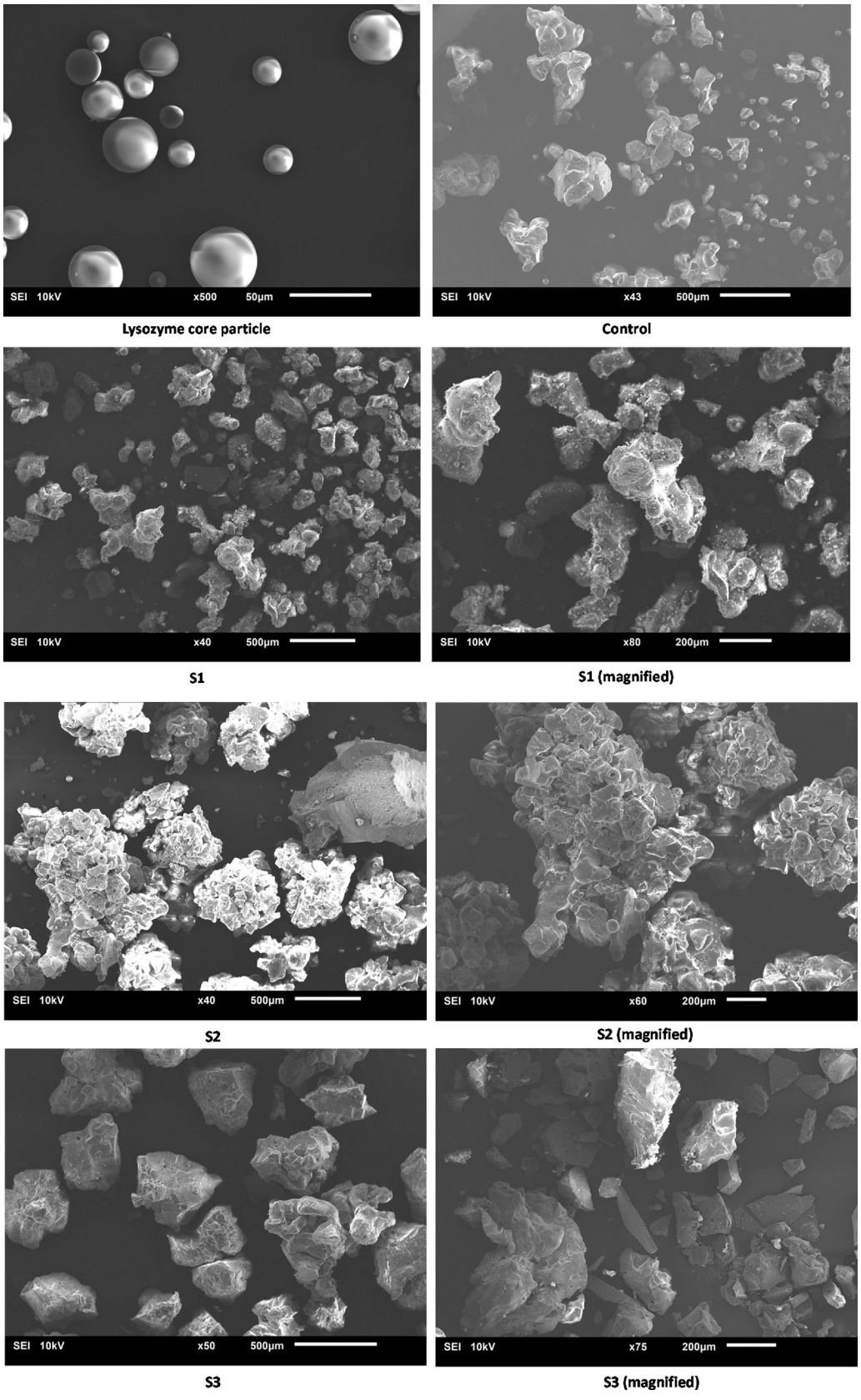

Fig. 4. SEM images of core lysozyme particles to be coated in the PSSC process (see Fig. 1 and text for details), Control sample (with water spraying instead of DS spraying) and products from PSSC process (sample S1, S2 and S3) with DS spraying. A magnified image of S1 shows that there are small particles deposited onto the surface of large particles. The magnified image of S2 shows that the big particles are clusters of particles with a size in the same magnitude order as that in S1 and S3. SEM images of S1 at higher magnifications are provided in the supplementary materials (Supplementary figures and tables, Fig. 2).

Control sample, protein without DS, showed an immediate lysozyme release both in water and in PBS, where 100% protein release was already measured at first time point. In water, where the ionic strength is low, the release of lysozyme from the S3 particles was limited to about 20% after 4 days, while in PBS, a quick lysozyme burst release of about 70% was detected after 1 h and a cumulative release up to 90% was reached after 4 days.

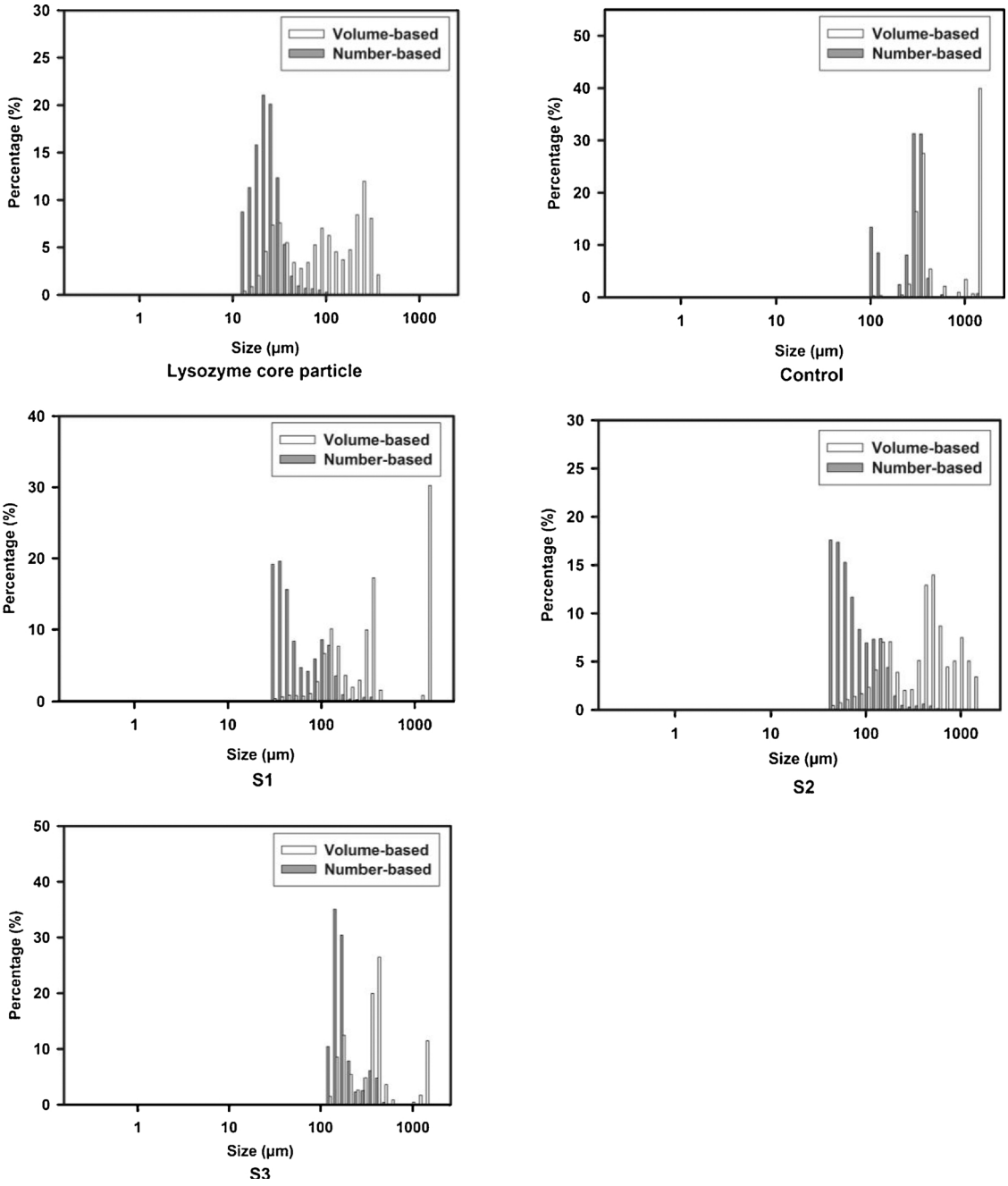

Fig. 5. Particle size distribution, measured in dry mode by laser diffraction, of lysozyme core particles, Control sample and sample S1, S2 and S3 produced via PSSC process.

Table 2
Residual moisture content of samples of the PSSC process.

Sample	Moisture content (%)
Lysozyme core particles	2.5 ± 1.1
Control	3.0 ± 0.7
S1	3.4 ± 1.1
S2	3.1 ± 0.8
S3	4.9 ± 0.5

Table 3
Zeta-potential of lysozyme, DS and product of PSSC process.

	Mean zeta potential (mV)[a]	Standard deviation (mV)[b]	Zeta deviation (mV)[c]
Lysozyme	34.4	7.6	19.2
DS	−42.6	2.3	19.7
Control	16.0	5.9	25.5
S1	−20.8	3.5	21.3
S2	−6.4	2.4	30.9
S3	−5.9	1.5	42.6

[a] Average zeta-potential of triplicate measurements.
[b] Standard deviation of the mean zeta-potential of triplicate measurements.
[c] A zeta-potential deviation reported by Malvern Nano-zetasizer, representing the distribution of zeta-potential contributed from differently charged particles [38].

4. Discussion

4.1. Influence of the spraying conditions on particle coating

4.1.1. Optimal spraying droplet size

A small (DS) droplet size with a homogeneous size distribution of

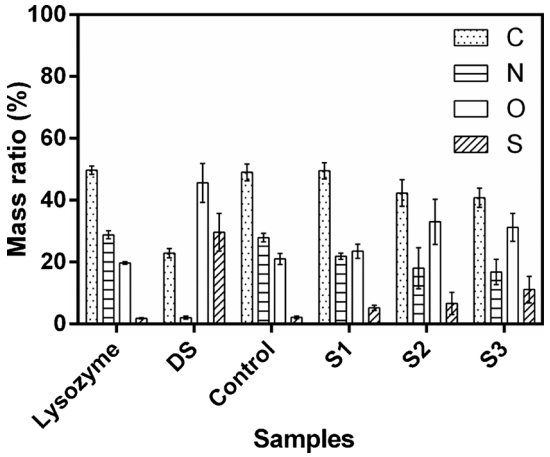

Fig. 6. Elemental composition of lysozyme, DS and products of PSSC process detected by EDS at an accelerating voltage of 10 kV.

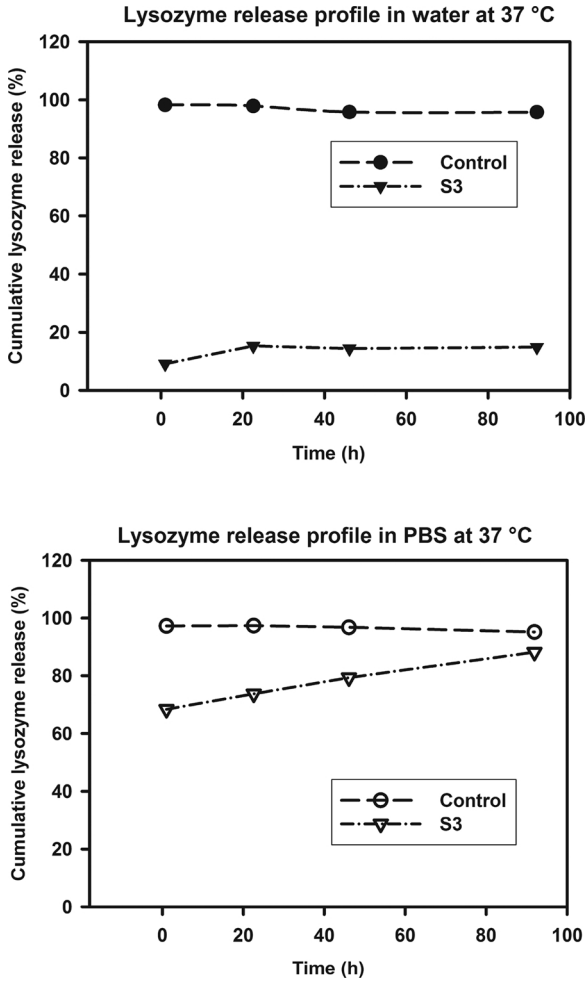

Fig. 7. Lysozyme release profile from the Control and S3 sample particles in water and PBS at 37 °C.

dissolved coating material is expected to give optimal coating [33,44–46]. According to previous literature [47] on the correlation between spraying droplet size and favourable particle coating, it is predicted that the size of droplets must be smaller than that of the core particle (micrometre range) in order to obtain the coating of the core particles with relatively little agglomeration.

Due to the closed high-pressure system, the droplet size could not be observed directly. Therefore, an effort was made here to derive the droplet size indirectly. The size of the dispersed DS droplets was determined based on the size of the spray-dried DS particles. When assuming that one droplet creates one primary DS particle by the process of drying, a mass balance allows calculating the original droplet size.

According to the number based particle size distribution, the majority of the spray dried DS particles ranged in size from 2 to 15 µm, with an average size of about 5 µm. DS particles have a density of about 1.96 g/cm^3 [48] and the 10% (w/w) DS solution has a measured density of about 1.05 g/cm^3 (via an Anton Paar DMA 5000 density meter (data not included)). If it is assumed that both the droplets and the spray-dried particles have a spherical shape, the size of the dispersed DS droplets can be calculated to be been between 5 and 40 µm.

In order to assess whether the dispersed DS droplets had been already completely dried before their contact with the core particles, a simple mass transfer simulation based on Fick's law using Comsol Multiphysics software was conducted, using the diffusion coefficients of water and $scCO_2$ in the corresponding medium that were reported before [49,50]. The simulation results are displayed in the supplementary materials (Supplementary figures and tables, Fig. 5). Based on this simulation, theoretically in fresh $scCO_2$, it takes about 0.5 ms to 20 ms for the sprayed DS droplet to be dried. The spraying $scCO_2$ flow rate is about 30 m/s at the nozzle tip, and the travel distance for the dispersed droplets for the contact with suspending particles is about 10 cm, corresponding to a residence time of approximately 3 ms. This means that part of the DS particles may be pre-dried before their contact with the solid core lysozyme particles.

A small number fraction of the spray dried DS particles has a large size of hundreds of micrometres, suggesting that the original droplet size is even bigger. These large droplets should dry slowly in $scCO_2$ and may be one of the factors leading to possible re-dissolution and misshaping of micro core particles or formation of bridges and agglomerates among them, as reflected by the SEM images of the samples (see Fig. 4).

The average size of the sprayed DS droplets (number-based) is about half the average size of the core particles (about 20 µm). This suggests that the majority of the dispersed droplets are smaller than those of the core particle, which should be favourable for the coating of core particles [47].

4.1.2. DS spraying flow rate and residual moisture content

This study aims to produce DS-encapsulated lysozyme particles with the help of $scCO_2$. In the PSSC process, the $scCO_2$ flow rate was always 300 g/min while the DS solution injection flow rate was varied from 0.2 ml/min to 1 ml/min in the different experiments. In general, at small volumes of liquid with large volumes of gas using twin-fluid nozzles, a higher liquid flow rate tends to lead to larger droplet sizes [51], implying that the droplet size can be controlled by varying the gas-to-liquid mass ratio (GLR) through the nozzle [52]. From this we expect to generate larger droplets at higher DS solution flow rates.

Larger droplets may also form by coalescence of the dispersed droplets before drying and the larger droplets will take longer to dry due to the limited mass transfer in the water-$scCO_2$ binary system. If the droplets cannot leave the system through the paper filter at the bottom of the vessel (something which is not known), this might lead to an increase of the hold-up of water in the vessel.

These combined phenomena resulted in a higher residual moisture content of the particles at a DS flow rate of about 1 ml/min (GLR ≈ 300) (about 5% (w/w) moisture content) compared to that at flow rate of 0.2 and 0.5 ml/min (GLR = 1500 and 600, respectively; about 3-3.5% moisture content; see Table 2).

At equal flow rates (1 ml/min), the residual moisture content of the particles for the Control experiment with only water spraying is lower (about 3%) than for that of S3 (about 5%). This is probably related to the approximately 20% higher viscosity, and slightly lower (about 6%) surface tension of the 10% DS solution (see Supporting figures and tables, Table 1), giving rise to larger droplets during the atomisation

and to reduced transport rates. Moreover, the amount of water bound to DS may also contribute to the difference of the residual moisture. Less than 2 water molecules are bound per sugar ring onto DS [48], representing an amount of residual water of less than 0.08 g for the 1 g of sprayed DS. This would theoretically add maximally 4% to the moisture content of the (complex) protein particles, so this might explain the higher moisture content of S3 compared to the Control (no DS).

4.2. Composition of produced particles and efficacy of the coating

The present study was meant to learn whether lysozyme core particles could be coated with DS through the PSSC process. According to the SEM images, spherical core lysozyme particles (see Fig. 4) agglomerate into larger particles during the PSSC process. Only few original lysozyme particles are still present in the Control sample (with the addition of just water in the absence of DS), and mainly new, agglomerated particles are visible in which the original spherical shapes of the lysozyme core particles are hardly present anymore. This might be explained from a dissolution-growth mechanism. Such a process probably also takes place in the presence of DS (see Fig. 4, S1, S2 and S3), in addition to the coating of the core lysozyme by DS.

Whether the protein core particles were indeed coated by DS was evaluated by both the zeta-potential and the elemental composition on the top layer of the product microparticles.

Zeta-potentials of the samples from the PSSC process were measured (in ethanol) and compared with the measured values for lysozyme (about +34 mV) and DS (about −43 mV). The reverse of the zeta-potential from positive to negative values indicates that there is DS present at the particle surface.

For S1, a low DS injection flow rate was used. According to the discussion in 4.1.1, this low DS flow rate may lead to a pre-drying of DS before it comes in contact with or coats the lysozyme core particles (see Supplementary figures and tables, Fig. 2). During the zeta-potential measurement, those DS particles which were more loosely attached to the agglomerates, contribute to the broad zeta-deviation and tend to shift the mean zeta-potential to more a negative value. The samples from the PSSC process contain particles that differ greatly in size, morphology and composition (i.e., lysozyme to DS ratio), which will give rise to different zeta-potential values.

EDS analyses were performed to learn whether the particles from the PSSC process were partly coated by DS. In this study, S was regarded as the representative element of DS. DS has a theoretical S content of 15% (w/w) compared to 2% for lysozyme, and the measured values were 30% and 2%, respectively. Theoretically lysozyme contains 20% N with 29% measured. Through calculations based on the S and N mass contents and the mass ratios of C and O to the representative elements, a mixture of DS and lysozyme was detected on the top layer of the S1, S2 and S3 sample particles whereby the detected DS content of S3 was higher than that of S1 and S2.

Based on the morphology of the product samples, the zeta-potential and EDS analysis, it can be concluded that mixed particles can be produced consisting of lysozyme and DS. However, a conclusion on the homogeneity and completeness of the core particle coating in the PSSC process cannot be drawn yet.

4.3. Protein release behaviour from the produced particles

Retarded protein release is the final target of the DS coated lysozyme particles obtained via the PSSC process. When suspending the DS-containing PSSC processed particles (S3) in PBS, after one hour about 70% of the lysozyme was released in the solution. When placed in water, however, this initial release was much less (about 10%). One factor causing the burst release of lysozyme is the dissolution of pure protein particles. The product particles of S3 exhibited about 10% less initial (i.e. after 1 h) burst release in PBS than those of S1 and S2 (see Supplementary figures and tables, Fig. 4), where S3 had a higher DS content than S1 and S2. The protein Control sample without DS dissolved completely in one hour.

The much faster release at the higher ionic strength of the PBS, compared to water was expected [1] and is probably due to a weakened electrostatic interaction between lysozyme and DS.

After the initial burst release, a slow release stage followed. Since the Control sample did not have such a slow phase, this slow release stage has to be related to the DS. It apparently hampers the dissolution or the diffusion of the protein, by binding to it or by forming a layer around the protein particle [53–55]. Such a shell type layer would swell when the particle comes into contact with the water and forms a diffusion barrier.

As for the lysozyme release in S1 and S2, after exposing the particles *in vitro to* PBS for about two days, a decrease of free dissolved lysozyme was detected (see Supplementary figures and tables, Fig. 4). Complexation of released lysozyme with free polyelectrolyte may account for the detected decrease of the lysozyme concentration [56].

The product particles from the PSSC process formulated with DS show some slow release behaviour. To prolong the release of lysozyme, a next step could be to treat the DS formulated particles with a cationic hydrophilic polymer such as DEAE-dextran (diethylaminoethyl-dextran hydrochloride). This polymer might form a layer on top of a possible DS layer of the current product particles and the newly-formed particles are expected to exhibit slower release profiles. Thicker layers might be constructed by repeated DS-DEAE-dextran layer deposition.

5. Conclusion

In this study, a $scCO_2$ spray coating process was developed to demonstrate the possibility of coating lysozyme core particles by hydrophilic polyelectrolyte. Core microparticles agglomerated into larger particles during the process, pointing at the interaction between solid protein particles and polymer droplets. Zeta-potential and EDS analysis indicate that DS was deposited onto or mixed with lysozyme in the agglomerated product particles. In some cases, a reduced lysozyme release rate was observed for the product particles, compared to the Control (no DS). This study lays the foundation for the achievement of layer-by-layer encapsulation of protein particles via $scCO_2$ processes.

Acknowledgement

This work was supported by the Netherlands Organisation for Scientific Research (NWO) Domain Applied and Engineering Sciences (TTW) [grant number 12144], which is partly funded by the Ministry of Economic Affairs.

Appendix A. Supplementary data

Supplementary data associated with this article can be found, in the online version, at https://doi.org/10.1016/j.supflu.2017.12.014.

References

[1] N. Kamiya, A.M. Klibanov, Controling the rate of protein release from polyelectrolyte complexes, Biotechnol. Bioeng. 82 (2003) 590–594.
[2] T.M. Allen, P.R. Cullis, Drug delivery systems: entering the mainstream, Science 303 (2004) 1818–1822.
[3] V. Sinha, A. Trehan, Biodegradable microspheres for protein delivery, J. Controlled Release 90 (2003) 261–280.
[4] Z. Antosova, M. Mackova, V. Kral, T. Macek, Therapeutic application of peptides and proteins: parenteral forever? Trends Biotechnol. 27 (2009) 628–635.
[5] S. Mitragotri, P.A. Burke, R. Langer, Overcoming the challenges in administering biopharmaceuticals: formulation and delivery strategies,Nature reviews, Drug Discovery 13 (2014) 655.
[6] Y. Yeo, N. Baek, K. Park, Microencapsulation methods for delivery of protein drugs, Biotechnol. Bioproc. Eng. 6 (2001) 213–230.
[7] M. van de Weert, W.E. Hennink, W. Jiskoot, Protein instability in poly (lactic-co-glycolic acid) microparticles, Pharm. Res. 17 (2000) 1159–1167.
[8] J. Patil, M. Kamalapur, S. Marapur, D. Kadam, Ionotropic gelation and

polyelectrolyte complexation: the novel techniques to design hydrogel particulate sustained, modulated drug delivery system: a review, Digest J. Nanomater. Biostruct. 5 (2010) 241–248.
[9] Z. Liu, Y. Jiao, Y. Wang, C. Zhou, Z. Zhang, Polysaccharides-based nanoparticles as drug delivery systems, Adv. Drug Deliv. Rev. 60 (2008) 1650–1662.
[10] M. Prabaharan, J. Mano, Chitosan-based particles as controlled drug delivery systems, Drug Deliv. 12 (2004) 41–57.
[11] O. Pillai, R. Panchagnula, Polymers in drug delivery, Curr. Opin. Chem. Biol. 5 (2001) 447–451.
[12] W.R. Gombotz, D.K. Pettit, Biodegradable polymers for protein and peptide drug delivery, Bioconjugate Chem. 6 (1995) 332–351.
[13] T. Yamaguchi, Lipid microspheres as drug carriers: a pharmaceutical point of view, Adv. Drug Deliv. Rev. 20 (1996) 117–130.
[14] M. Hall, C. Ricketts, The use of dextran sulphate as a blood anticoagulant in biological research, J. Clin. Pathol. 5 (1952) 366–366.
[15] H.M. Bugg, P.H. King, C.W. Randall, Polyelectrolyte conditioning of alum sludges, J. (Am. Water Works Assoc.) (1970) 792–795.
[16] R. Bijlsma, A. Van Well, M.C. Stuart, Characterization of self-assembled multilayers of polyelectrolytes, Physica B 234 (1997) 254–255.
[18] A.L. Becker, A.P. Johnston, F. Caruso, Layer-By-Layer-Assembled capsules and films for therapeutic delivery, Small 6 (2010).
[19] Y. Lvov, K. Ariga, I. Ichinose, T. Kunitake, Layer-by-layer architectures of concanavalin A by means of electrostatic and biospecific interactions, Journal of the Chemical Society, Chem. Commun. (1995) 2313–2314.
[20] F. Caruso, D.N. Furlong, K. Ariga, I. Ichinose, T. Kunitake, Characterization of polyelectrolyte- protein multilayer films by atomic force microscopy, scanning electron microscopy, and Fourier transform infrared reflection- absorption spectroscopy, Langmuir 14 (1998) 4559–4565.
[21] N.K. Varde, D.W. Pack, Microspheres for controlled release drug delivery, Expert Opin. Biol. Ther. 4 (2004) 35–51.
[22] S. Lankalapalli, V. Kolapalli, Polyelectrolyte complexes: a review of their applicability in drug delivery technology, Indian J. Pharm. Sci. 71 (2009) 481.
[23] N. Jovanović, A. Bouchard, G.W. Hofland, G.-J. Witkamp, D.J. Crommelin, W. Jiskoot, Stabilization of proteins in dry powder formulations using supercritical fluid technology, Pharm. Res. 21 (2004) 1955–1969.
[24] O. Nuchuchua, H. Every, G. Hofland, W. Jiskoot, Scalable organic solvent free supercritical fluid spray drying process for producing dry protein formulations, Eur. J. Pharm. Biopharm. 88 (2014) 919–930.
[25] M.J. Whitaker, J. Hao, O.R. Davies, G. Serhatkulu, S. Stolnik-Trenkic, S.M. Howdle, K.M. Shakesheff, The production of protein-loaded microparticles by supercritical fluid enhanced mixing and spraying, J. Controlled Release 101 (2005) 85–92.
[26] K. Mishima, K. Matsuyama, D. Tanabe, S. Yamauchi, T.J. Young, K.P. Johnston, Microencapsulation of proteins by rapid expansion of supercritical solution with a nonsolvent, AIChE J. 46 (2000) 857–865.
[27] I.R. Dos Santos, J. Richard, B. Pech, C. Thies, J. Benoit, Microencapsulation of protein particles within lipids using a novel supercritical fluid process, Int. J. Pharm. 242 (2002) 69–78.
[28] F. Jordan, A. Naylor, C. Kelly, S. Howdle, A. Lewis, L. Illum, Sustained release hGH microsphere formulation produced by a novel supercritical fluid technology: in vivo studies, J. Controlled Release 141 (2010) 153–160.
[29] Y. Kang, C. Yang, P. Ouyang, G. Yin, Z. Huang, Y. Yao, X. Liao, The preparation of BSA-PLLA microparticles in a batch supercritical anti-solvent process, Carbohydr. Polym. 77 (2009) 244–249.
[30] T.J. Young, K.P. Johnston, K. Mishima, H. Tanaka, Encapsulation of lysozyme in a biodegradable polymer by precipitation with a vapor-over-liquid antisolvent, J. Pharm. Sci. 88 (1999) 640–650.
[31] L.S. Tu, F. Dehghani, N. Foster, Micronisation and microencapsulation of pharmaceuticals using a carbon dioxide antisolvent, Powder Technol. 126 (2002) 134–149.
[32] J. Kluge, F. Fusaro, N. Casas, M. Mazzotti, G. Muhrer, Production of PLGA micro- and nanocomposites by supercritical fluid extraction of emulsions: i. Encapsulation of lysozyme, J. Supercrit. Fluids 50 (2009) 327–335.
[33] A. Palamanit, S. Prachayawarakorn, P. Tungtrakul, S. Soponronnarit, Performance evaluation of top-Spray fluidized bed coating for healthy coated rice production, Food Bioprocess Technol. 9 (2016) 1317–1326.
[34] S.R. Werner, J.R. Jones, A.H. Paterson, R.H. Archer, D.L. Pearce, Air-suspension particle coating in the food industry: part I—State of the art, Powder Technol. 171 (2007) 25–33.
[35] T.N. Zwietering, Suspending of solid particles in liquid by agitators, Chem. Eng. Sci. 8 (1958) 244–253.
[36] F. Caruso, H. Möhwald, Protein multilayer formation on colloids through a stepwise self-assembly technique, J. Am. Chem. Soc. 121 (1999) 6039–6046.
[37] L.E. Bromberg, A.M. Klibanov, Transport of proteins dissolved in organic solvents across biomimetic membranes, Proc. Natl. Acad. Sci. 92 (1995) 1262–1266.
[38] U. Nobbmann, Zeta deviation larger than the mean – how can that be? (2015) [cited 2017 18 September]; Available from: http://www.materials-talks.com/blog/2015/09/24/zeta-deviation-larger-than-the-mean-how-can-that-be/.
[39] A. Sophianopoulos, C. Rhodes, D. Holcomb, K. Van Holde, Physical studies of lysozyme I. characterization, J. Biol. Chem. 237 (1962) 1107–1112.
[40] M.M. van Beers, C. Slooten, J. Meulenaar, A.S. Sediq, R. Verrijk, W. Jiskoot, Micro-Flow Imaging as a quantitative tool to assess size and agglomeration of PLGA microparticles, Eur. J. Pharm. Biopharm. 117 (2017) 91–104.
[41] H. Nagendra, C. Sudarsanakumar, M. Vijayan, An X-ray analysis of native monoclinic lysozyme. A case study on the reliability of refined protein structures and a comparison with the low-humidity form in relation to mobility and enzyme action, Acta Crystallogr., Sect D: Biol. Crystallogr. 52 (1996) 1067–1074.
[42] Dextran Sulphate Product Information, Sigma-Aldrich, 2017.
[43] U. Cheema, Standardisation in Cell and Tissue Engineering: Methods and Protocols, Woodhead publishing, 2013.
[44] S. Maronga, On the Optimization of the Fluidized Bed Particulate Coating Process, Kemiteknik, 1998.
[45] V. Saini, Fluidized bed processing for multiparticulates, J. Chem 2 (2009) 447–450.
[46] K. Dewettinck, A. Huyghebaert, Top-spray fluidized bed coating: effect of process variables on coating efficiency, LWT-Food Sci. Technol. 31 (1998) 568–575.
[47] M. Mishra, Handbook of Encapsulation and Controlled Release, CRC Press, 2015.
[48] S. Lüsse, K. Arnold, Water binding of polysaccharides NMR and ESR studies, Macromolecules 31 (1998) 6891–6897.
[49] B. Xu, K. Nagashima, J.M. DeSimone, C.S. Johnson, Diffusion of water in liquid and supercritical carbon dioxide: an NMR study, J. Phys. Chem. A 107 (2003) 1–3.
[50] S.P. Cadogan, G.C. Maitland, J.M. Trusler, Diffusion coefficients of CO2 and N2 in water at temperatures between 298.15K and 423.15K at pressures up to 45MPa, J. Chem. Eng. Data 59 (2014) 519–525.
[51] K. Omer, N. Ashgriz, Spray nozzles, Handbook of Atomization and Sprays, Springer, 2011, pp. 497–579.
[52] K. Masters, Spray Drying Handbook, Spray Drying Handbook, (1985).
[53] M. George, T.E. Abraham, Polyionic hydrocolloids for the intestinal delivery of protein drugs: alginate and chitosan—a review, J. Controlled Release 114 (2006) 1–14.
[54] I.-C. Liao, A.C. Wan, E.K. Yim, K.W. Leong, Controlled release from fibers of polyelectrolyte complexes, J. Controlled Release 104 (2005) 347–358.
[55] S. Shu, C. Sun, X. Zhang, Z. Wu, Z. Wang, C. Li, Hollow and degradable polyelectrolyte nanocapsules for protein drug delivery, Acta Biomater. 6 (2010) 210–217.
[56] S. Mehrotra, D. Lynam, R. Maloney, K.M. Pawelec, M.H. Tuszynski, I. Lee, C. Chan, J. Sakamoto, Time controlled protein release from layer-by-Layer assembled multilayer functionalized agarose hydrogels, Adv. Funct. Mater. 20 (2010) 247–258.